Richards Equation–Based Modeling to Estimate Flow and Nitrate Transport in a Deep Alluvial Vadose Zone

Article *in* Vadose Zone Journal · November 2012

DOI: 10.2136/vzj2011.0145

CITATIONS
53

READS
345

4 authors, including:

Thomas Harter
University of California, Davis
241 PUBLICATIONS **6,101** CITATIONS

SEE PROFILE

Published November 28, 2012

Special Section: Model-Data Fusion in the Vadose Zone

Farag E. Botros
Yuksel S. Onsoy
Timothy R. Ginn
Thomas Harter*

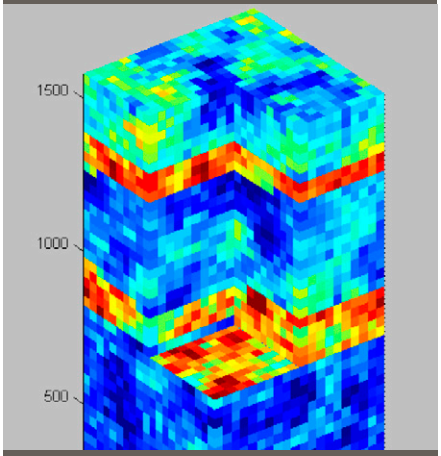

Long-term fate of nitrate in well-characterized, deep, unsaturated heterogeneous alluvial sediments is simulated with several Richards' equation-based flow and transport models (deterministic and stochastic). Results consistently overestimate field-measured nitrate calling into question the appropriateness of these models.

F.E. Botros, Y.S. Onsoy, and T. Harter, Land, Air, and Water Resources, University of California, Davis, CA 95616; T.R. Ginn, Civil & Environmental Engineering, University of California– Davis, CA 95616. F.E. Botros, also at Irrigation and Hydraulics Department, Faculty of Engineering, Cairo University, Orman, Giza 12613–Egypt and currently at Daniel B. Stephens & Associates, Inc. Albuquerque, NM 87109; Y.S. Onsoy, currently at Kennedy/Jenks Consultants, San Francisco, CA 94107. *Corresponding author (thharter@ucdavis.edu).

Vadose Zone J.
doi:10.2136/vzj2011.0145
Received 11 Jan. 2011.

Richards Equation–Based Modeling to Estimate Flow and Nitrate Transport in a Deep Alluvial Vadose Zone

Heterogeneity in unsaturated soils and sediments is well known to exist at different scales, from microscopic scale to macroscopic scale. Characterization of different types of heterogeneity in deep vadose zones is challenging because of the usual lack of information at such sites. In this paper, we considered a site with detailed geological, chemical, and hydraulic properties measurements throughout an approximately 16-m deep vadose zone consisting of unconsolidated, alluvial deposits typical for the alluvial fans of the eastern San Joaquin Valley, California. At the agricultural site, data were also available for a 7-yr long field fertilization experiment that we used to independently estimate the amount of nitrate stored within the vadose zone at the end of the experiment. Simple mass balance calculations were performed and compared to six conceptually different two-dimensional and three-dimensional vadose zone numerical models that were implemented to represent varying degrees of hierarchical details of heterogeneity. Despite widely differing structure and heterogeneity of unsaturated flow, all models resulted in a narrow range of estimated nitrate storage in the deep vadose zone for near-cyclically repeated water and nitrogen fertilizer applications. Simulated nitrate storage was found to be approximately six to eight times larger than the measured storage at the field. Simulated nitrate variability, while qualitatively similar in pattern, was considerably lower than measured, despite the large simulated hydraulic variability. This study underscores that physical heterogeneity of deep vadose zones may have limited effects on the transfer of conservative contaminants applied repeatedly to the land surface. It also raises questions about our understanding of the chemical fate of nitrate in the vadose zone; and suggests the presence of a significant immobile moisture domain within the deep vadose zone that is not explainable by heterogeneity of Richards equation parameters, yet needs to be considered for simulating nitrate transport under conditions of cyclical infiltration with gravity dominated convective flux.

Fertilizers, salts, and pesticides continue to be a major source of nonpoint-source pollution in agricultural areas. Our knowledge of vadose zone properties is essential to assess the long-term impacts of nitrogen fertilizer management practices on groundwater quality, especially in agricultural groundwater basins of California and similar semiarid regions where irrigation return flow is a major component of recharge to local groundwater systems. The threat of nitrate to the groundwater of the Central Valley of California has recently been highlighted by the United Nations, in a national study, and in a California study (United Nations, 2011; Dubrovsky et al., 2010; Harter et al., 2012). The understanding of processes in the deep vadose zone is a critical factor in designing efficient nutrient management protocols (Ling and El-Kadi, 1998). These protocols aim to enhance agricultural production while protecting groundwater from nitrate contamination.

A considerable amount of research has been applied to study the nitrogen mass balance in the root zone (e.g., Lafolie et al., 1997; de Vos et al., 2000; Allaire-Leung et al., 2001; Stenger et al., 2002). Nitrogen budgeting in the root zone has been widely used in agronomy to determine the fate of N in soils and the potential for N leaching to groundwater. It is commonly thought that the vadose zone below the root zone acts as a limited buffer zone where nitrate is partially or fully attenuated by denitrification before reaching groundwater. Contrarily, non-uniform, heterogeneous flow with low-resistance flow paths in the vadose zone might occur and have been thought to expedite nitrate leaching in the deep vadose zone and accelerate nitrate arrival to groundwater (Ünlü et al., 1990; Harter and Yeh, 1996; Simunek et al., 2003; Baran et al., 2007).

The effect of fate and transport processes in the vadose zone below the root zone on nitrate leaching to groundwater is still not adequately quantified. Spatial variability in the deep vadose zone below the root zone is rarely characterized or mostly unaccounted for in most groundwater quality assessment studies, due to costs and technical difficulties in sampling heterogeneous soil, and in monitoring deep nitrate over long temporal scales. However, few studies have been guided by and compared to actual, extensive field data from a deep vadose site (Rockhold et al., 1996; Seong and Rubin, 1999).

We have described a deep vadose zone field research site that is ideally suited for testing various heterogeneity models and their associated transient, long-term flow and transport predictions against actually measured two- and three-dimensional profiles (Onsoy et al., 2005; Harter et al., 2005). Our project site is a former orchard on the alluvial fan of the Kings River in the eastern San Joaquin Valley, Fresno, CA. The orchard was subject of a long-term, 12-yr field scale nitrogen fertilizer experiment. Spatial variability of the site is well characterized throughout the 16-m deep vadose zone (Botros et al., 2009) and the site is typical of many alluvial basins in California. Data from the fertilizer experiment, site characterization, and description of the hydraulic parameters heterogeneity are found in Onsoy et al. (2005) and Botros et al. (2009) and are the foundation for the model development presented in this paper.

The intensive field sampling campaign employed by Onsoy et al. (2005) showed that the stored nitrate mass (based on 1200 soil core samples) below the root zone is, first, highly variable, and second, much lower than expected from agronomic water and root zone nitrogen mass balance considerations. That led to the hypothesis that, given the strong heterogeneity observed at the site, significant preferential or non-uniform flow paths might have occurred, facilitating accelerated nitrate movement through the deep vadose zone to the water table with much lower N mass left behind in the vadose zone. Denitrification as the main cause for low vadose zone N storage was not supported as measured data did not indicate that a significant gradient existed in the vertical N mass profile nor was a significant increase in ^{15}N composition found with depth (Harter et al., 2005).

To test the hypothesis that heterogeneity is a primary control on nitrate transport and occurrence and to better understand the role of heterogeneity in nitrate transport through a deep alluvial vadose zone, we describe the development of six different conceptual modeling approaches using findings of statistical and geostatistical analysis of hydraulic parameters performed recently (Botros et al., 2009). We compare various conceptual models of heterogeneity in both, two-dimensional and three-dimensional simulation domains.

Specifically, we (i) evaluate the impact of spatial variability observed at the site at two scales- lithofacies and local scale- on variations in water flow conditions and on nitrate distribution in the deep vadose zone, (ii) test the hypothesis that the stronger heterogeneity leads to lower observed nitrate mass in the deep vadose zone through more non-uniform flow and accelerated transport, and (iii) test if the Richards equation can provide such non-uniform flow paths under conditions of infiltration with gravity/pressure gradient dominated convective flux.

This paper is structured as follows. The Site Description section gives a brief description of the site and highlights the main findings of our sampling analysis. The Model Development section provides mathematical background on the flow and solute transport in the unsaturated zone. The Model Application section explains the main elements in the development of the different conceptual models. The Results section then presents the results of these different conceptual models, the Discussion section discusses the results, and the Conclusion section summarizes the study and highlights main conclusions.

Site Description

Details of the field site characterization efforts have been described in Harter et al. (2005) and in Onsoy et al. (2005). Briefly, the site is a former orchard of 'Fantasia' nectarines, about 0.8 ha (2 acres) located at the University of California, Kearney Agricultural Center, (http://www.uckac.edu, accessed 2 Oct. 2012), on the Kings River alluvial plain, 30 km southeast of Fresno, CA. As in many other surrounding areas, over the past four decades groundwater levels at the orchard have fluctuated between approximately 11 m and 21 m below the surface with an average thickness of the unsaturated zone of approximately 16 m. The site elevation is 103 m above sea level and has a semiarid, Mediterranean climate.

From 1982 until 1994, a fertilizer experiment was conducted in a random block design to 14 different subplots at the site with application rates of 0, 110, 195, 280, or 365 kg N ha^{-1} yr^{-1} in several replicates (Johnson et al., 1995). In 1997, three subplots within the 0, 110, and 365 kg N ha^{-1} yr^{-1} treatments were selected for sampling. For convenience, the three subplots are named throughout the text as "control," "standard," and "high," respectively. Between July and October 1997, 62 undisturbed continuous soil cores were drilled to the water table at a depth of 15.8 m and soil samples were collected for the analysis of nitrate and hydraulic parameters distributions (Onsoy et al., 2005; Botros et al., 2009). Soil texture at the core scale was determined by the hydrometer method (Sheldrick and Wang, 1993); soil hydraulic properties were determined using the multi-step outflow method (Eching and Hopmans, 1993); and field soil water content was determined gravimetrically (Klute, 1986). Based on texture, color, and cementation encountered in the cores, eight, statistically significant, different stratigraphic units or layers were identified and are hereinafter referred to as *lithofacies* (Botros et al., 2009).

The entire vadose zone at the site consists of unconsolidated sediments deposited on a stream-dominated alluvial fan. Textural groups range from clay, clayey paleosol hardpans to a wide range of

silt and sand, occasionally coarse sand and highly localized gravel sediments. Lithofacies exhibit vertically varying thicknesses; similar sediment deposits are laterally continuous across the experimental site. Lithofacies units identified here are depicted in Fig. 1 and they include from the ground surface toward the water table: upper Hanford sandy loam (SL1), sand (S1), shallow hardpan (P1), sandy loam unit (SL2), sand (S2), clay/clayey silt/clay loam (C-T-L), lower sandy loam (SL3), and a deep hardpan or paleosol (P2). Geologic formation and sedimentologic description and details on characteristics of each of these lithofacies are found in (Botros et al., 2009).

Model Development

Governing Equations for Flow

Based on the continuum concept and the REV approach, simulation of water flow in variably saturated media at the laboratory scale uses the classical Richards equation here written for isotropic three-dimensional flow:

$$\frac{\partial \theta}{\partial t}=\frac{\partial}{\partial x}\left[K(h)\frac{\partial h}{\partial x}\right]+\frac{\partial}{\partial y}\left[K(h)\frac{\partial h}{\partial y}\right]+\frac{\partial}{\partial z}\left[K(h)\left(\frac{\partial h}{\partial z}+1\right)\right]-S_w \quad [1]$$

where θ is the volumetric water content [–], t is the time [T], h is the soil water matric head [L], x, y, and z are the spatial coordinates [L], and S_w is a sink term which represents the volume of water removed per unit time from a unit volume of soil [T^{-1}]. $K(h)$ is the unsaturated hydraulic conductivity [$L\ T^{-1}$].

A number of closed-form formulas have been proposed to empirically describe the dependence of hydraulic functions $K(h)$ and $\theta(h)$ on pressure head (Brooks and Corey, 1964; Gardner, 1958; Haverkamp et al., 1977; Russo, 1988). Here, we use those of Mualem (1976) and van Genuchten (1980):

$$K(h)=K_s S_e^{l}\left[1-\left(1-S_e^{1/m}\right)^{m}\right]^2 \quad [2a]$$

$$S_e=\frac{\theta(h)-\theta_r}{\theta_s-\theta_r}=\left[1+|\alpha h|^{n}\right]^{-m} \quad [2b]$$

where K_s denotes the saturated hydraulic conductivity [$L\ T^{-1}$], S_e [–] is called effective water saturation ($0 \le S_e \le 1$), θ_s and θ_r [–] are the saturated and residual water content, respectively, and α [L^{-1}], m(–), and n [–] are empirical parameters dependent on soil type where $m = 1 - 1/n$ and l denotes tortuosity/connectivity coefficient [–] which is found to have a value of 0.5 from the analysis of a variety of soils (Mualem, 1976).

Governing Equations for Solute Transport

The classic advection-dispersion equation for transport is here adopted to account for mixing and spreading of an inert solute during transient simulations:

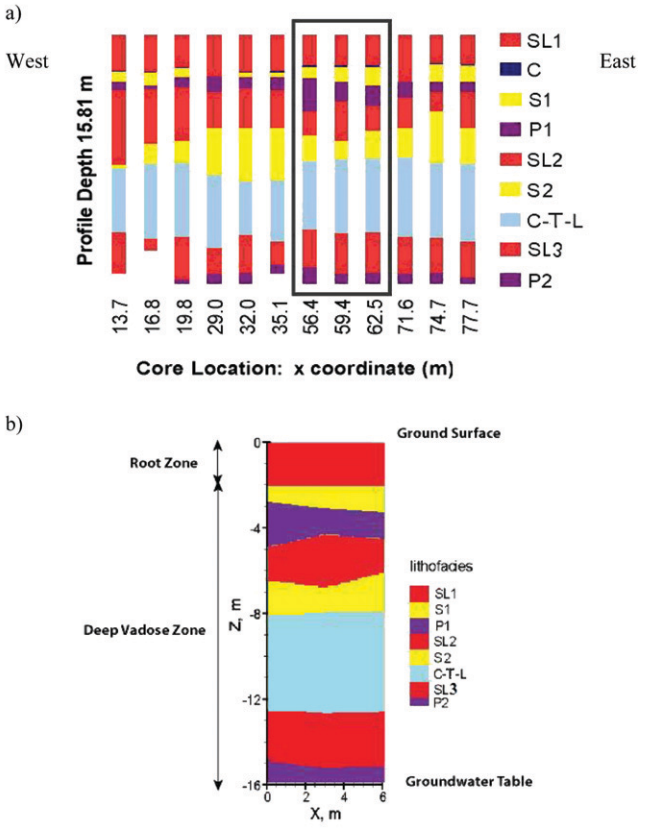

Fig. 1. (a) East–west lithofacies cross-section identified at the fertilizer experimental site; (b) typical cross-section that is used in the numerical model.

$$\frac{\partial \theta C}{\partial t}=\frac{\partial}{\partial x_i}\left(\theta D_{ij}\frac{\partial C}{\partial x_j}\right)-\frac{\partial q_i C}{\partial x_i} \quad [3]$$

where C is the local concentration in the soil solution [$M\ L^{-3}$], x_i are spatial coordinate (i = 1, 2, 3) [L], q_i is the ith component of water flux density [$L\ T^{-1}$], and D_{ij} is the hydrodynamic dispersion coefficient tensor [$L^2\ T^{-1}$] (i, j = 1,2, 3). Knowledge of water content, θ, and water flux density, q_i, is obtained from solutions of the Richards and Darcy's equations. The hydrodynamic dispersion coefficient D_{ij} tensor, which describes the combined effect of mechanical dispersion and molecular diffusion, is given by (Scheidegger, 1960):

$$D_{ij}=(\alpha_L-\alpha_T)\frac{v_i v_j}{v}+\alpha_T v\delta_{ij}+D_o \quad [4]$$

Where α_L and α_T are longitudinal and transverse dispersivities, respectively, v is the magnitude of pore water velocity, δ_{ij} is the Kronecker delta ($\delta_{ij} = 1$ if $i = j$, and $\delta_{ij} = 0$ otherwise), and D_o is molecular diffusion.

HYDRUS (Simunek et al., 1996) was used to numerically simulate the movement of water and nitrate in the unsaturated zone. The

program solves three-dimensional Richards equation (Eq. [1]) and the three-dimensional advection-dispersion equation for transport (Eq. [3]) using Galerkin-type linear finite element schemes with the mass conservative iterative scheme proposed by Celia et al. (1990). Detailed documentation on the software can be found elsewhere (Simunek et al., 1996; Rassam et al., 2003).

Model Application

Model Domain and Boundary Conditions

Most of the soil cores were clustered in three subplots at the field site (Botros et al., 2009). Lithofacies sequences along an E–W transect of the drilled soil cores were analyzed and were found to be relatively continuous across the site; however, variable lithofacies thicknesses were observed (Fig. 1a). Three of these cores were combined here to build a typical cross-section of the heterogeneous vadose zone profile at the site (Fig. 1b) and used for our numerical modeling simulations. The cross-section has a width of 6.1 m and a depth of 15.8 m (depth to the water table). In three-dimensional models, the model domain is extended in the lateral horizontal direction and domain dimensions were 6.1 by 6.1 by 15.8 m.

For the flow problem, atmospheric boundary conditions were assigned to the top of the domain prescribing daily values of water fluxes including precipitation, irrigation, and evapotranspiration. At the bottom of the domain, a constant pressure of h = 0 cm was imposed, representing the long-term average water table position at 15.8-m depth. For the transport problem, a third type (Cauchy) boundary condition was specified along the upper boundary to define N mass flux into the domain through fertilizer applications. Here, we consider all nitrogen to be applied in form of nitrate, not subject to sorption or chemical reactions. A second type (Neumann) boundary condition was prescribed at the bottom boundary, where N mass was directed out of the domain at the water table. Concentration data did not indicate a strong horizontal flow regime leading to highly stratified concentrations (no significant vertical trend was observed in the field data). Hence, vertical domain boundaries were assumed to be symmetry boundaries, simulated as zero flux boundary conditions for both flow and transport simulations.

Precipitation and Irrigation Inputs

Daily values of precipitation from 1990 to 1996 were obtained from a weather station located within 1 km from the site. The station (No. 39-Parlier) is managed by the California Irrigation Management Information System (CIMIS) (http://www.water.ca.gov/wateruseefficiency/, accessed 2 Oct. 2012). Based on the 7 yr of data, the average annual precipitation is 37 cm. In most years, essentially no precipitation was recorded between May and early October.

Throughout the experiment, flood irrigation, common for many orchards in the project area, was performed usually from April through September. Dates of irrigation events were tabulated for the simulation duration of 1990–1996 (Table 1). The number of annual irrigation applications at the orchard varies from 9 to 17 with an average of 13 irrigations per year. Based on site records, the amount of water applied, at each irrigation application, is an average of 13.44 cm. Irrigation duration is approximately 20 h while irrigation frequency varies between few days to few weeks depending on crop growth stage.

Evapotranspiration

Evapotranspiration (ET) defines a combination of two separate processes whereby water is lost from the soil surface by evaporation and from the root zone by crop transpiration. Reference evapotranspiration, ET_o, taken as potential ET for a grass (or alfalfa) that

Table 1. Records of irrigation applications at the fertilizer subplots from 1990 to 1996. Variations reflect climatic variations with more irrigations following dry winters (e.g., 1992) and irrigation management decisions.

Irrigation no.	1990	1991	1992	1993	1994	1995	1996
1	29 March	7 February	22 April	19 March	21 March	1 May	1 May
2	17 April	3 May	29 April	16 April	14 April	10 May	9 May
3	8 May	22 May	7 May	5 May	10 May	22 May	21 May
4	4 June	4 June	18 May	18 May	23 May	31 May	3 June
5	14 June	20 June	28 May	1 June	1 June	8 June	25 June
6	21 June	1 July	3 June	9 June	9 June	20 June	2 July
7	27 June	15 July	9 June	18 June	16 June	3 July	30 July
8	3 July	30 July	18 June	24 June	23 June	10 July	11 September
9	10 July	8 August	25 June	1 July	30 June	25 July	3 October
10	24 July	6 September	1 July	9 July	16 July	7 August	
11	9 August		8 July	19 July	28 July	23 August	
12	5 September		23 July	30 July	8 August	6 September	
13	18 September		6 August	9 August	16 September	4 Octocber	
14			20 August	24 August			
15			31 August	2 September			
16			10 September	14 September			
17			28 September				

does not suffer water stress, was predicted using climatologic data (DWR, 2001). Reference evapotranspiration is a climatic parameter and computed from weather data including solar radiation, air temperature, air humidity and wind speed. Daily ET_o data with grass as the reference crop was readily available from the local CIMIS meteorological station (No. 39-Parlier, Fresno County). Crop evapotranspiration was calculated through the estimation of the crop coefficient, which is dependent on crop characteristics, vegetative growth stage, canopy cover and height as well as soil surface properties (Doorenbos and Pruitt, 1977). HYDRUS requires evapotranspiration pre-partitioned into two components: evaporation and transpiration. Evaporation is controlled by the water content and hydraulic gradient at the soil surface layer and it is essentially important in the early stages of crop development. Transpiration, on the other hand, is distributed over the root zone and can be limited to plant roots by soil water availability. A dual crop coefficient method (Allen et al., 1998) has been used to split evapotranspiration into the two separate components. Annual potential evaporation, averaged over 7 yr, was calculated as 17 cm, which was about 15% of the annual potential evapotranspiration of 111 cm.

Nitrogen Application

Nitrogen was always applied to the subplots, during fertilizer application, in the form of ammonium-nitrate. The vast majority of ammonium-nitrate was applied during late fall when trees were dormant similar to the practice in orchards of California and of other fruit-growing regions (Weinbaum et al., 1992). Ammonium-nitrate was expected to be nitrified and converted to nitrate rapidly (Ünlü et al., 1999). Given our observation horizon of multiple years, initial time needed for N transformations and their effects on root N uptake were considered negligible. Dates and amounts of fertilizer applications at the standard and high subplots were tabulated for the simulation period (Table 2). In addition to nitrogen applied to the soil during fertilization, nitrogen was also added through irrigation water. Average NO3–N concentration in irrigation water was taken to be 4.0 mg L^{-1} (Harter et al., 1999). Thus, each irrigation application supplied approximately 5.4 kg N ha^{-1}.

Root Zone

Plant water uptake and plant nutrient uptake occur in the plant root zone. Approximately 90% of the tree roots in the nectarine orchard occur within the uppermost 1.8 m (Onsoy et al., 2005). Thus, an average of 1.8 m was used to represent the depth of the tree root zone.

Plant Water Uptake

In our application, the sink term, S_w in Eq. [1] represents the volume of water removed per unit time from a unit volume of soil due to plant water uptake. Feddes et al. (1978) defined S_w as

$$S_w(h) = \gamma(h) S_p \quad [5]$$

where the water stress response function $\gamma(h)$ is a prescribed dimensionless function of the soil water pressure head ($0 \leq \gamma \leq 1$), and S_p is the potential water uptake rate [T^{-1}] and is calculated as T_p/L_z where T_p [$L\ T^{-1}$] is the transpiration obtained from partitioning ET data and L_z is the depth of root zone (1.8 m in this case).

Plant Nitrogen Uptake

There are two major mechanisms involved in the nutrient uptake by plants: active uptake and passive uptake (Hopmans and Bristow, 2002). The passive nutrient uptake represents the mass flow of nutrient into roots with water while active nutrient uptake represents the movement of nutrients into the roots induced by other mechanisms than mass flow (Simunek and Hopmans, 2009). Active uptake dominates in the low supply concentration range, while passive uptake and diffusion across the membrane becomes more important in the high concentration range (Hopmans and Bristow, 2002). In this experiment, nitrate was always abundant for plants and the majority of nutrient uptake is expected to occur through passive uptake. This approach has been applied in practice to account for plant uptake of nutrients in other numerical models (e.g., Vogeler et al., 2001).

Table 2. Records of fertilizer applications at the fertilizer subplots from 1990 to 1996. N concentrations are evaluated based on the amount of surface water flux that entered the model that day (irrigation, I, or precipitation, P, or both, I+P).

Year	Dates of fertilizer application	Subplot†	Applied N	Flux type entering the model‡
			kg ha^{-1}	
1990	29 March	H	85	I
	8 May	H	85	I
	4 June	H	85	I
	18 September	S/H	110	I
1991	22 March/23March§	H	85	P
	3 May	H	85	I
	4 June	H	85	I + P
	6 September	S/H	110	I
1992	20 March	H	85	P
	29 April	H	85	I
	28 May	H	85	I
	10 September	S/H	110	I
1993	19 March	H	85	I
	5 May	H	85	I
	1 June	H	85	I
	14 September	S/H	110	I
1994	21 March	H	85	I
	10 May	H	85	I
	1 June	H	85	I
	16 September	S/H	110	I
1996	11 September	S/H	110	I

† S/H: Fertilizer applied both on the standard and high subplots; H: fertilizer applied on the high subplot.
‡ I: Fertilizer applied by irrigation water; P: fertilizer applied by precipitation; I+P: fertilizer by irrigation and precipitation.
§ Fertilizer applied by precipitation in two consecutive days.

Initial Conditions

Initial distribution of water content or pressure head at the site was not readily available. We established a pressure profile between the ground surface and the water table by applying the analytical method proposed by Rockhold et al. (1997) and as was presented previously in Onsoy (2005). This method solves the Richards equation for one-dimensional, heterogeneous layered systems under a steady state flux at the ground surface. We applied the method to our flow domain composed of eight horizontal layers. Boundaries of these layers were defined based on the average thicknesses of lithofacies identified at the field. Steady state flux was estimated as 0.23 cm d^{-1} from long-term (14 yr) records of site precipitation, evapotranspiration, and average annual irrigation. The pressure profile varies within the layers as a function of the soil hydraulic properties of each layer (Fig. 2).

Unsaturated Soil Hydraulic Properties

The extensive deep vadose zone sampling campaign at the site provides one of only a few extensive datasets available to date, to the best of our knowledge, for evaluating a model with a more refined characterization of the subsurface heterogeneity. In an attempt to better simulate the subsurface geology and the corresponding soil hydraulic properties, six numerical models were developed to simulate transient flow and nitrate transport through the 15.8-m thick vadose zone in which three of these models were two-dimensional and the other three were three-dimensional. In these numerical models, three conceptual modeling approaches were used to represent three different levels in simulated heterogeneity complexity: (i) a homogenous lithofacies model (HM-2D and HM-3D) representing large scale heterogeneity only, (ii) a heterogeneous lithofacies model with spatially variable scaling factors (HetSF-2D and HetSF-3D), and (iii) a heterogeneous lithofacies model with spatially variable van Genuchten (VG) parameters (HetVG-2D, and HetVG-3D). The latter four of the six conceptual models represent both large-scale and small-scale heterogeneity, or in other words a lithofacies-scale heterogeneity (a few meters in thickness and tens of meters in lateral extent) and local-scale heterogeneity (a few centimeters in thickness and a few decimeters in width). The six models were used to determine the dependence of the nonuniformity of flow and nitrogen content in the deep vadose zone on the dimensionality and level of heterogeneity represented in the model. In all two-dimensional models, the longitudinal dispersivity (α_L) was assumed to be 10 cm and the transverse dispersivity (α_T) was assumed to be 1 cm. In three-dimensional models, and due to larger domain discretization, α_L and α_T were set to 20 cm and 2 cm, respectively.

Homogeneous Lithofacies Model (HM)

As the vadose zone was composed of distinct layers (Fig. 1), the assumption of relative homogeneity of soil hydraulic properties for each layer is a common practice to delineate different layers of soil texture, in unsaturated flow and transport problems (Hills et al., 1991; Roth et al., 1991; Nimmo et al., 2002; Zhu and Mohanty, 2002).

The HM model conceptualizes each lithofacies of the eight main lithofacies as a homogenous unit with soil hydraulic parameters defined using the van Genuchten model and treated as constant deterministic values within each lithofacies. Mean VG parameters of each lithofacies can be found in Botros et al. (2009) and boundaries of each lithofacies are shown in Fig. 1b. This model only considers *between-lithofacies* or *large-scale* heterogeneity while *within-lithofacies* or *small-scale* heterogeneity is neglected. In the three-dimensional models and due to the lack of information in the N–S transect, layer boundaries in the N–S direction were assumed to be oriented strictly horizontal.

Heterogeneous Lithofacies using Scaling Factors

In contrast to the HM approach, small scale variability was taken into account in the HetSF approach through scaling analysis. Scaling is a technique used to simplify the analysis of hydraulic parameter datasets in heterogeneous unsaturated sediments. It is based on the concept that the various hydraulic parameters, e.g., K_s, α, n, θ_s, θ_r, are all related to the pore size distribution and pore geometry (Miller and Miller, 1956). As the pore geometry varies with the type of sediment, the various hydraulic parameters vary accordingly. The scaling factor (λ) is a measure of that change in pore geometry. It relates the actual hydraulic function derived for a sample to the scaled hydraulic function. Scaling factors were obtained from hydraulic analysis of 120 soil core samples from 19 soil cores drilled to 16 m (Botros et al., 2009). Scaling factors were found to follow a lognormal distribution which was consistent with other studies (Warrick et al., 1977; Rao and Wagenet, 1985; Vachaud et al., 1988; Hopmans et al., 1988; Tseng and Jury, 1994; Braud et al., 1995). The mean value of ln (λ) was found to be −1.28 and the standard deviation of ln (λ) was 1.07.

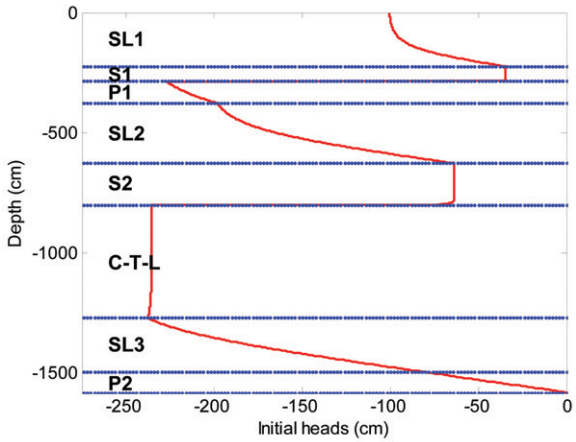

Fig. 2. Initial condition pressure profile established for the eight-layered soil domain under a steady flux of 0.23 cm d^{-1}.

Previously, only a few studies analyzed scaling factors with geostatistical tools (Jury et al., 1987; Russo, 1991; Zavattaro et al., 1999). In this study, geostatistical analysis of scaling factors was implemented. Lithofacies boundaries were considered geostatistical discontinuities and no spatial correlation was assumed across lithofacies boundaries. Horizontal and vertical semivariograms were constructed and fitted to spherical covariance function. The horizontal and vertical spherical semivariograms constructed for scaling factors were used to define the degree of spatial variability. Scaling factors in both horizontal and vertical directions did not exhibit strong spatial continuity. The vertical semivariogram showed a spatial continuity with a range of 1.5 m which is close to the average lithofacies thickness while the horizontal semivariogram did not show much spatial continuity and was assumed to have a range of half the sampling interval (coincidentally also 1.5 m).

Statistical and geostatistical analysis were used to generate a random field of scaling factors to be used in our numerical simulations (Fig. 3). Consistent with the lithofacies textures (Botros et al., 2009), high values of scaling factors coincided within the coarse-textured materials (S1 and S2), whereas low values were generated within other lithofacies that all have relatively fine texture. Spatial continuity in the E–W direction was also used to extend the generated random field in the N–S direction for the sake of generating a random field realization to be used in the three-dimensional model simulation (Fig. 3).

Heterogeneous Lithofacies using van Genuchten Parameters (HetVG)

Oliveira et al. (2006) demonstrated in principle that when hydraulic parameters are all related to each other through a single variable, such as scaling factors, the resulting unsaturated flow and transport variability is significantly underestimated. We therefore also implemented the HetVG approach, which, like the HetSF approach, takes into account small-scale heterogeneity in addition to the large-scale heterogeneity. In the HetVG approach, however, separate random fields of K_s, α, and n were generated based on statistical and geostatistical analysis of hydraulic parameters data (Botros et al., 2009). Much larger horizontal continuity than vertical continuity can be observed for all parameters in the two-dimensional and three-dimensional simulation domains (Fig. 4). Within-lithofacies variability of θ_r and θ_s was found to be small and was therefore neglected.

Space and Time Discretization

For two-dimensional simulations using the HM and HetSF approaches, the domain was discretized into square cells with dimensions $\Delta x = \Delta z \approx 15$ cm. In the HetVG approach, and because of high nonlinearity in the parameter values associated with this approach, the domain was discretized through cells with dimensions $\Delta x = \Delta z = 10$ cm. In the three-dimensional simulations, all model conceptualization domains were discretized into cells with dimensions $\Delta x = \Delta y = \Delta z \approx 30$ cm. All simulations ran for 7 yr (from 1 Jan. 1990 through 31 Dec. 1996). During the simulations, time step size Δt was automatically controlled according to the convergence history (e.g., the maximum change in pressure head and water content during each time step).

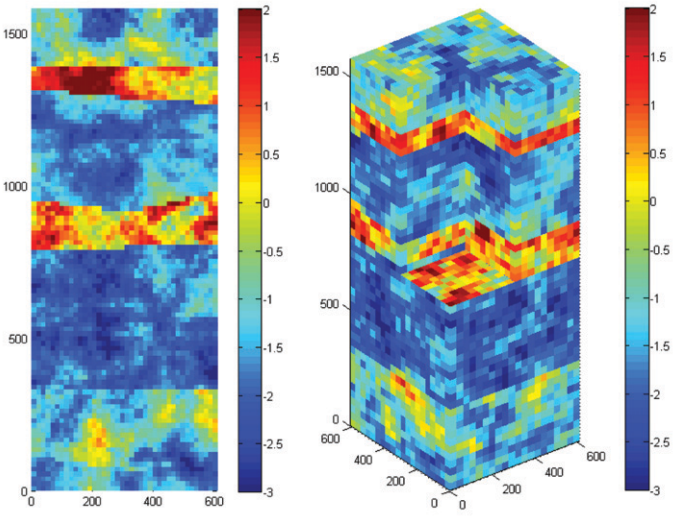

Fig. 3. Distribution of ln (λ) in two-dimensional and three-dimensional model domains:.

Results

A relative water mass balance error of less than 2% was achieved in all model runs. Among the simulations, the heterogeneous lithofacies models (i.e., HetSF and HetVG) were computationally more expensive and produced slightly higher mass balance errors than the homogeneous lithofacies model. HM-2D ran in approximately 45 min on a dual-core processor at 2.66 GHz with

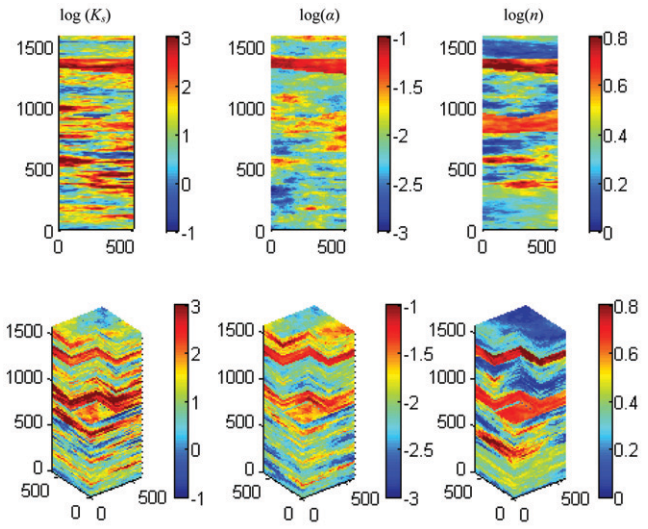

Fig. 4. Distribution of log K_s, log α, and log n in the two-dimensional and three-dimensional heterogeneous van Genuchten model conceptualization. Top row: two-dimensional simulations. Bottom Row: three-dimensional simulations.

3.25GB of RAM. CPU times for simulating HM-3D, HetSF-2D, HetSF-3D, HetVG-2D, and HetVG-3D were 1.5, 2, 8, 10, and 50 times longer, respectively.

Nitrogen mass balance errors at the standard and high subplots fluctuated from near zero to 2% during the first 4 yr and reached a stable condition of approximately 0.2% in the HM and 0.5% in HetSF and HetVG during the latter years of simulation. Peclet number (P_e) and Courant number (C_r) criteria were used to control numerical oscillations and numerical dispersion during simulations. A commonly accepted stability criterion of $P_e C_r \leq 2$ was fulfilled throughout the simulation period (Simunek et al., 1996) in all simulation runs. Only slight differences were observed between the HM-2D and HM-3D approaches. This is expected due to the fact that these two simulations are conceptually identical with HM-3D being merely a lateral extrusion of HM-2D.

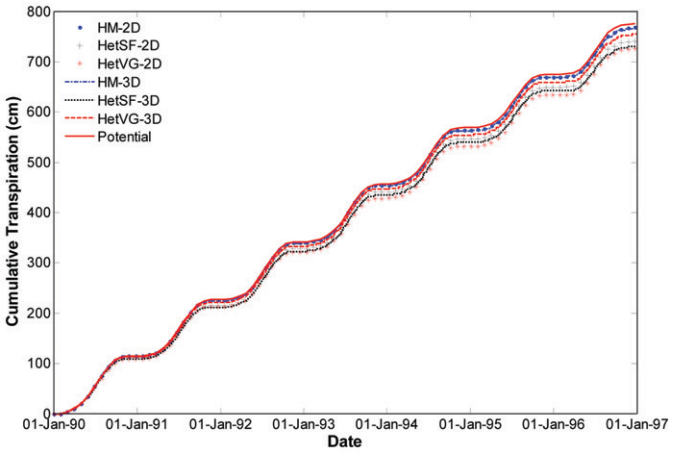

Fig. 5. Comparison of daily values of potential and model simulated (actual) transpiration during the simulation period (1990–1996) in all models.

Plant Water and Nitrogen Uptake

In all models, simulated transpiration is smaller than the prescribed potential transpiration. The reduction is the result of limited root zone water availability for tree water uptake. Simulated transpiration at the end of the 7-yr period in the two-dimensional simulations ranges from 94 to 99% of potential transpiration suggesting that water is mostly available for plants (Fig. 5).

Plant N uptake estimated by all models agree well with each other, suggesting that model dimensionality and root zone heterogeneity have limited effect on simulated plant N uptake. HetVG-2D results in slightly lower uptake and HetVG-3D results in slightly higher uptake than other simulations. In contrast, the effect of fertilizer treatment is significant. Total N uptake estimated by the end of the simulation period at the standard subplot is much less than the uptake amount at the high subplot (Fig. 6). At the standard subplot, average annual plant N uptake, estimated by all models, is 69 kg N ha^{-1}. At the high subplot, average annual N uptake value is 113 kg N ha^{-1}. These model estimates are reasonably close to the 7-yr average annual measured plant N uptake of 77 kg N ha^{-1} and 98 kg N ha^{-1}at the standard and high subplots, respectively (Onsoy et al., 2005).

Water and Nitrogen Flux at the Water Table

Water flux to the water table differed substantially between the six simulations at the beginning of the simulation (Fig. 7). These differences are believed to be a result of the simplifications implied in the initial conditions. After the first simulation year, differences in water flux to the water table between all models became negligibly small, at least at the seasonally and annually compounded scale (Fig. 7). In all models, gravity drainage throughout the unsaturated zone dominated the unsaturated flow. Driven by the highly transient surface fluxes, water flux at nearly 16-m depth (water table) is found to be also subject to temporally highly variable flow rates with seasonal and annual variations throughout the vadose zone despite its 14-m thickness below root zone. Each year, water flux peaks during the middle of summer, only a few months after the beginning of the irrigation season and starts declining with increasing water loss at the surface from evapotranspiration. Averaged across all models, annual peak fluxes vary from 0.36 cm d^{-1} in 1996 (with nine irrigations) to 1.5 cm d^{-1}in 1992 (with 17 irrigations).

Similar to water fluxes, cumulative N fluxes at the water table show only minor variations between the different models, except for the HetVG-3D simulation which has significantly lower N flux to the water table than other simulations, partly due to the higher N uptake in the root zone (Fig. 8).

Despite the differences in absolute N flux, the temporal dynamics of the N flux, such as timing of the onset of N-leaching at the water table and subsequent seasonal variations in N flux at the water table, are almost identical between simulations. Results vary significantly between fertilizer treatments (Fig. 8). At the end of

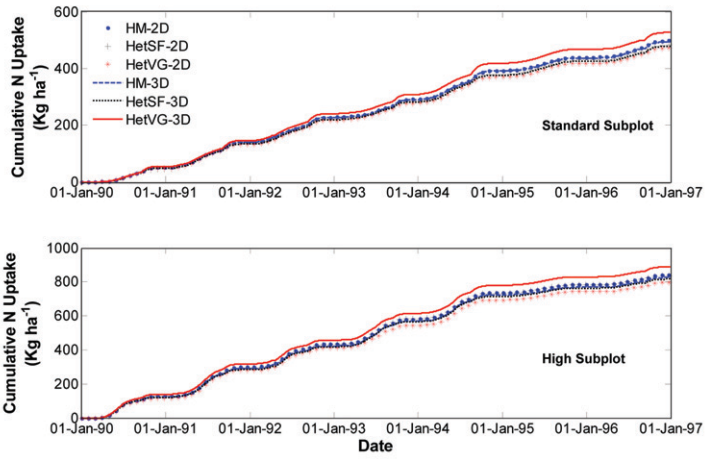

Fig. 6. Cumulative plant N uptake simulated at the standard and high subplots during the simulation period (1990–1996) in all models.

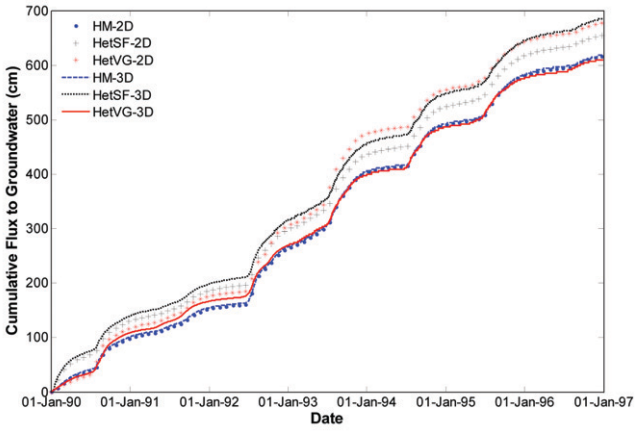

Fig. 7. Cumulative simulated water flux to the water table.

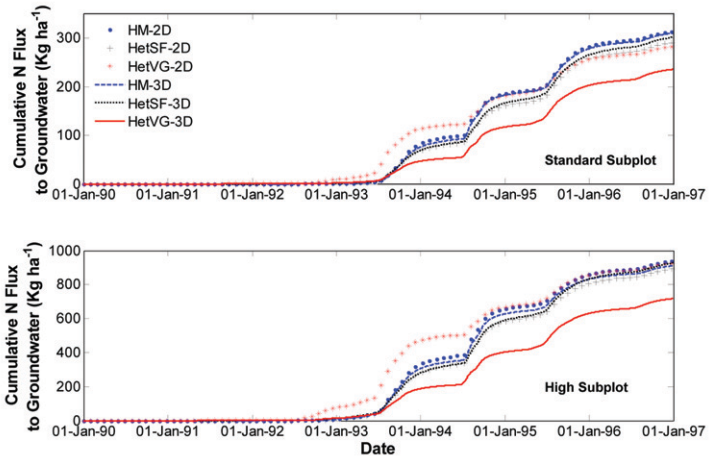

Fig. 8. Cumulative N flux at the water table (bottom of the 16-m thick simulation domain) of the standard and high subplots during the simulation period (1990–1996) in the homogeneous and heterogeneous lithofacies models.

the simulation, cumulative N flux at the water table of the high subplot is nearly three times that of the standard subplot.

Neither the fertilizer applications (standard or high) nor the model type (HM, HetSF, or HetVG), or the model dimensionality (two-dimensional or three-dimensional) showed a significant effect on the mean residence time of N in the vadose zone. This can be attributed to the strong uneven layering effect relative to the influence of local-scale heterogeneity. Similar results have been reported by Pan et al. (2009) who studied both layer-scale heterogeneity and local-scale heterogeneity in the unsaturated zone of Yucca Mountain, Nevada, and found that mean predictions were only slightly affected by the local-scale heterogeneity. According to Pan et al. (2009), more variability of first arrival at the water table was expected to be observed between simulations, as it is thought to be more significantly controlled by local scale heterogenity. In all our simulations, first arrival occurred approximately 3 yr after the beginning of the simulation. The discrepancy between the results of our simulations and those of Pan et al. (2009) is due to the fact that, in our experiment, N fluxes were mainly driven by the magnitude of irrigation fluxes prescribed at the surface and the large irrigation inefficiency at the site consistent with findings in other field experiments (e.g., Biggar and Nielsen, 1978; Wagenet and Hutson, 1989; Troiano et al., 1993). This underscores the importance of budgeting irrigation water in irrigated agriculture to mitigate downward movement of surface applied agrochemicals.

Pore Water Velocity Distribution in the Deep Vadose Zone

The geometric mean water velocity (Fig. 9) was calculated by taking an average on the log-10 transform of the pore water velocity in all model cells in the deep vadose zone (i.e., excluding the root zone). The geometric mean water velocity, while of measurably different magnitude between simulations, is mostly driven by the transient water flux out of the root zone. During the irrigation season, the mean velocity in all models is significantly larger than that between irrigation seasons. For the two-dimensional simulations, mean velocity and its variations in time are in good agreement between the three different models. Lower geometric mean velocities are observed with increasing (local) heterogeneity representation in the three-dimensional models, but temporal dynamics are very similar. Relative to the large seasonal fluctuations of velocity, differences in mean velocity between models are nearly negligible. This is consistent with the similarity in observed nitrate arrival times between the models. This further underscores the importance of large-scale (between lithofacies) heterogeneity over small-scale (within-lithofacies) heterogeneity on the field scale transport (Pan et al., 2009).

Back-transformed standard deviation of the log-10 transformed vertical pore water velocity are lowest in the homogeneous facies model, higher for the HetSF model, and highest for the HetVG model (Fig. 10). The latter two models yield significantly higher variability in the three-dimensional velocity field than the

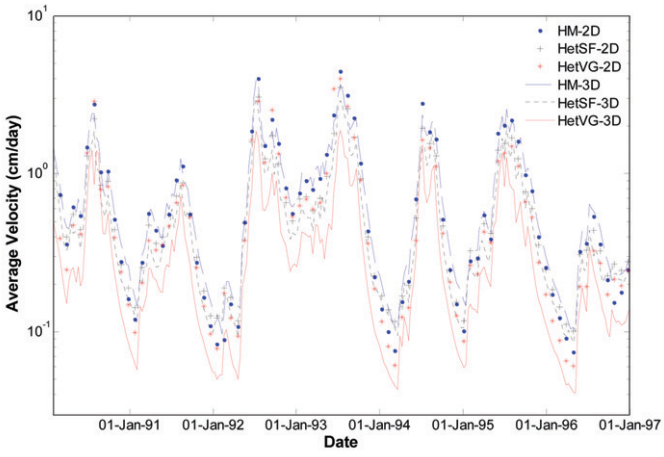

Fig. 9. Geometric mean of the vertical pore water velocity in each of the six models as a function of time. The mean is calculated over all deep vadose zone model cells (i.e., excluding the cells in the root zone).

two-dimensional velocity field. Seasonally, however, velocity variability remains relatively high at all times for the HetVF-3D model, while showing large seasonal fluctuation in the two-dimensional models and especially in the homogeneous facies (HM) model. In HetVG-3D, small-scale heterogeneity is the largest which is known to significantly contribute to the velocity standard deviation (e.g., Harter and Yeh, 1996; Pan et al., 2009).

With depth, velocities exhibit lithofacies-dependent means, but not a strong vertical trend, slightly decreasing for the arithmetic mean, slightly inceasing for the geometric mean (e.g., in HetVG-2D, the 7-yr geometric mean for SL1, S1, P1, SL2, C-T-L, SL3, and P2 is 0.20, 0.14, 0.30, 0.43, 0.51, 0.37, 0.66, and 0.63 cm d^{-1}, respectively). Lithofacies-dependent standard deviation of both velocity and log-10 transformed velocity also varies strongly by lithofacies, superimposed by some attenuation of variability with depth (for HetVG-2D, 7-yr back-transformed standard deviation of log-transformed velocity for SL1, S1, P1, SL2, C-T-L, SL3, and P2 is 3.6, 3.9, 2.0, 2.1, 3.2, 3.3, 2.4, and 1.5 cm/d, respectively).

Despite the similarity between the models in geometric mean velocity and in the magnitude of the velocity variations across the entire deep vadose zone, the patterns of the spatial velocity field distributions differ remarkably between the models. Smooth large-scale variations are observed in the HM model, while the visually most heterogeneous flux fields, with high tortuosity—large variations over short distances—occur in the heterogeneous three-dimensional models, especially the HetVG-3D models (Fig. 11), even suggesting preferential flow paths. Also, the HetVG-3D model exhibited strong relative variations across the velocity field during both low flow winter season and high flow summer season. In all models, existence of inclined layer boundaries between two adjacent layers and high hydraulic property contrast has significant impact on directing the flow. This is most pronounced in the HM model at the interface between SL2, a fine-textured layer, and S2, a coarse-textured layer, where a high velocity region is created at the boundaries between these two layers. Inclined layering has been shown to cause potential preferential flow paths (Kung, 1993).

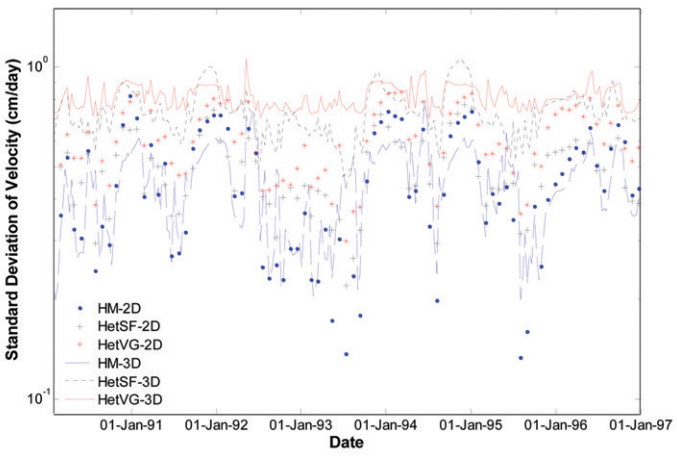

Fig. 10. Back-transformed standard deviation of log-base-10 transformed vertical pore water velocity as a function of time. Calculation is done over all deep vadose zone model cells (i.e., excluding the cells in the root zone).

In heterogeneous unsaturated media, flowpaths may significantly change between relatively dry drainage conditions and relatively wet infiltration conditions. Under wet conditions, coarse-textured regions provide the most conductive pathways, while, under drier conditions, finer-textured materials retain moisture and are relatively more permeable than coarse-textured, rapidly draining materials (Roth, 1995; Harter and Yeh, 1998). Comparison of flow regimes near the end of a very dry, non-irrigated period (January 1994) with the flow regime during a wet, irrigated period (July 1994) shows significant differences in the magnitude of the velocity field. However, at both (simulation) times, relatively higher velocity occur at the same lateral locations in the simulation domain. This suggests that, while significant drainage and drying occurs over the winter, the flow regime at this site does not change its relative position within the heterogeneous system at this alluvial site, given the frequent irrigations during the summer (Fig. 11).

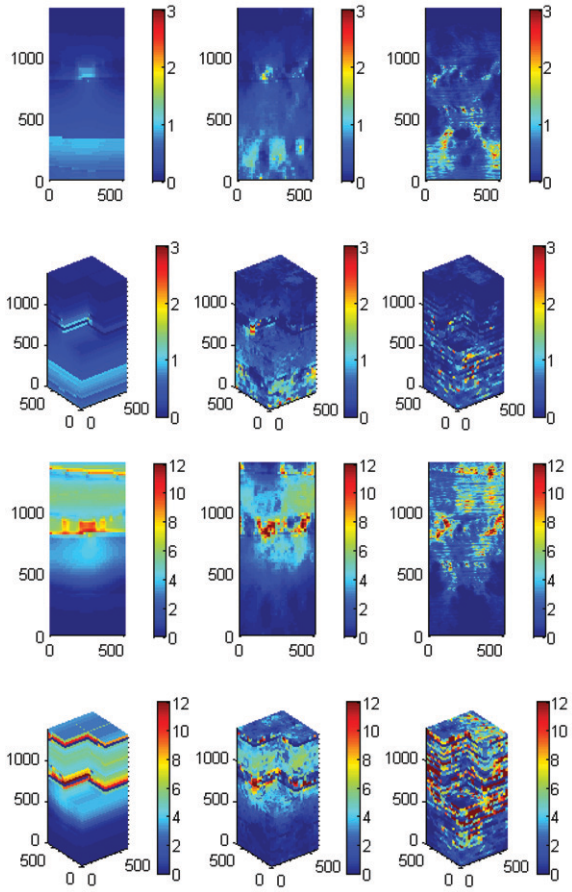

Fig. 11. Pore water vertical velocity (cm per day) in the deep vadose zone in January 1994 (top six panels) near the end of a long dry spell with no irrigation and in July 1994 (bottom six panels) during the middle of irrigation season with high flow rates to below the root zone. Within each six panel group: top row shows two-dimensional simulations and bottom row shows three-dimensional simulations. Left to right: HM, HetSF, and HetVG.

Nitrogen Concentration Distribution in the Deep Vadose Zone

Despite the visually much higher variability in the pore water velocity distribution in the models with local heterogeneities (Fig. 10 and 11), the average concentration—like the average pore velocity—did not show significant differences between the models. Lithofacies and depth have the most significantly control in all models (Fig. 12). Concentrations in shallow layers showed seasonal concentration differences between summer and winter seasons in response to seasonal nitrate and water releases from the root zone. However these differences diminished in deeper layers (Fig. 12).

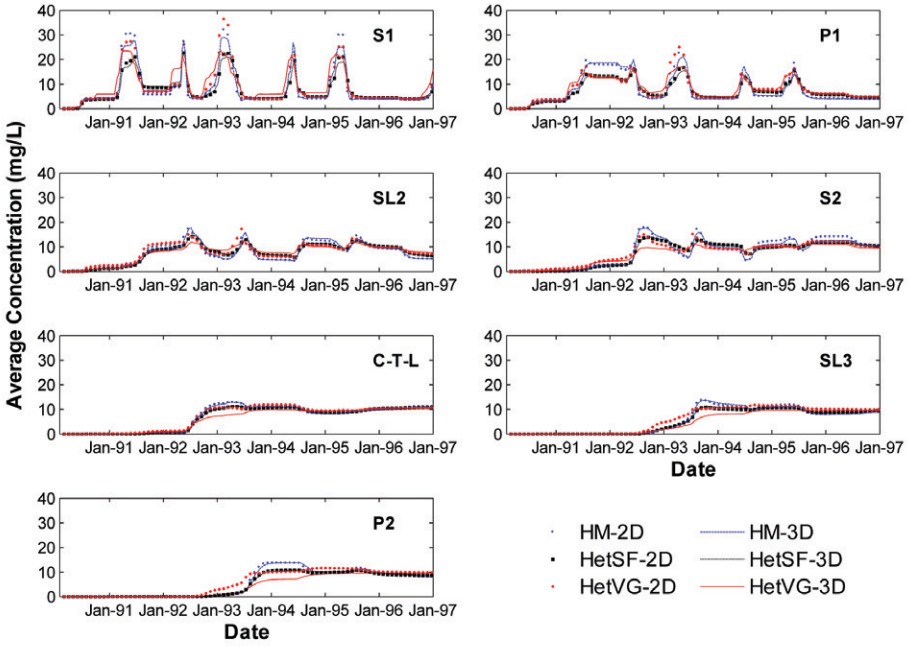

Fig. 12. Average concentration of nitrate N (mg L^{-1}) for the standard subplot for all lithofacies in the deep vadose zone (boundaries of lithofacies are depicted in Fig. 1). Top layer (SL1) was not plotted since most of it lies within root zone and it is more influenced by N uptake of roots.

The distribution of the simulated concentration across model cells below the root zone at the end of the simulation was found to be nearly log-normal distributed. In the HetVG-2D model, the maximum and minimum concentrations were approximately 42 mg L^{-1} and 3.9 mg L^{-1}, respectively, with more than half of all model cell concentrations between 9 mg L^{-1} and 12 mg L^{-1}. The log-normal distribution of the concentration is consistent with field measurements (Table 1 of Onsoy et al., 2005). However, in the field dataset, mean log nitrate concentrations is only about half of that simulated here. On the other hand, the average variance of the field nitrate samples (not including non-detects) is six times larger than in any of the model simulations. Importantly, nearly one-third of measured soil samples had nitrate concentrations below the detection limit (0.02 mg L^{-1}), while the simulations did not yield any concentration less than 3 mg L^{-1} at the end of the simulation period.

Figure 13 shows concentration distribution in all six models on 1 Jul. 1994, during the middle of irrigation season. Three major plumes corresponding to the three latest fertilization applications can be observed in the soil profile of all models. Nitrogen concentrations in HetSF and HetVG models exhibit significantly more longitudinal spreading than the HM model results. The highly non-uniform leading edge of N plumes indicates large variability in downward advances across the profile. Differences can be observed between concentration distribution in the two-dimensional and the three-dimensional simulations.

Total Nitrogen Mass in the Deep Vadose Zone

From 1990 to 1993, N mass in the deep vadose zone continues to increase at each subplot, resulting in a net accumulation of approximately 300 kg N ha^{-1} at the standard subplot and 800 kg N ha^{-1} at the high subplot. Starting in mid-1993, total N mass in the deep vadose zone remains relatively constant at the standard subplot with small annual fluctuations (Fig. 14). In the two-dimensional models, simulated total N mass in the deep vadose zone in the standard subplot after 7 yr of nitrogen management is 248 kg N ha^{-1}, 262 kg N ha^{-1}, and 268 kg N ha^{-1} for the HM, HetSF, and HetVG, respectively. Corresponding stored N mass for the high subplot are 534 kg N ha^{-1}, 565 kg N ha^{-1}, and 580 kg N ha^{-1}. For the three-dimensional models, corresponding values are 243 kg N ha^{-1}, 256 kg N ha^{-1}, and 287 kg N ha^{-1} for the standard subplot and 539 kg N ha^{-1}, 554 kg N ha^{-1}, and 614 kg N ha^{-1} for the high subplot. Neither the different modeling approaches nor the different model dimensionality explained the low N storage in the deep vadose zone observed in the field, which Onsoy et al. (2005) estimated to be 36 kg N ha^{-1} and 87 kg N ha^{-1} for the standard and high subplots, respectively.

Discussion

Numerical Modeling vs. Root Zone Mass Balance Approach

The root zone mass balance approach coupled with the plug flow assumption (Martin et al., 1991) is a most parsimonious model to predict mass transfer to groundwater. It assumes steady state flow in a one-dimensional representation of the vadose zone. Applying this simple concept to our field site (average annual deep percolation: 110 cm per year; average moisture content: 25%, Onsoy et al., 2005), estimated residence time of nitrate in the 14-m deep vadose zone is approximately 3.2 yr, similar to that estimated by the numerical two-dimensional and three-dimensional models

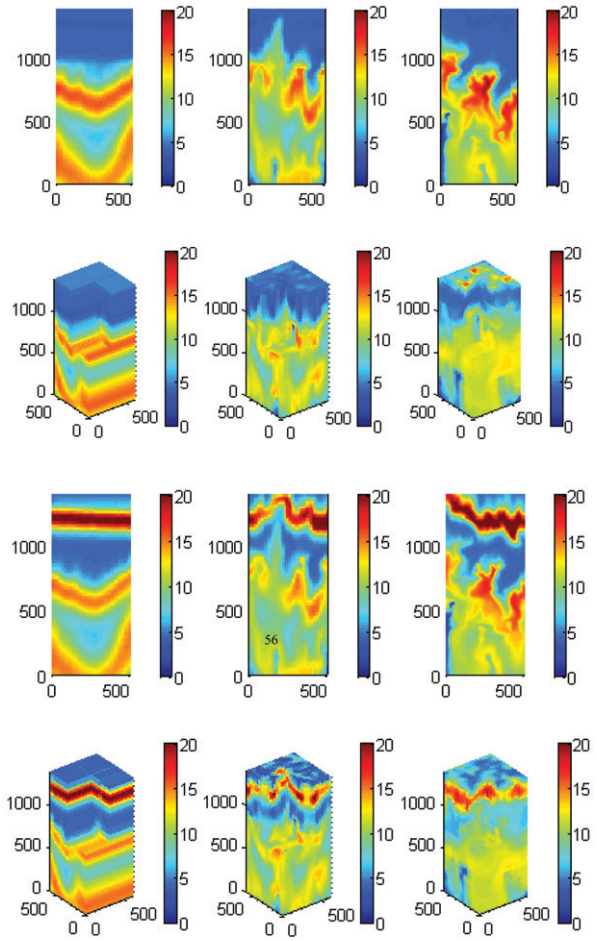

Fig. 13. Nitrate–N concentration (mg L^{-1}) for "standard subplot" in the deep vadose zone in January 1994 (top six panels) near the end of a long dry spell with no irrigation and in July 1994 (bottom six panels) during the middle of irrigation season with high water flow rates to below the root zone. Within each six panel group: top row shows two-dimensional simulations and bottom row shows three-dimensional simulations. Left to right: HM, HetSF, and HetVG.

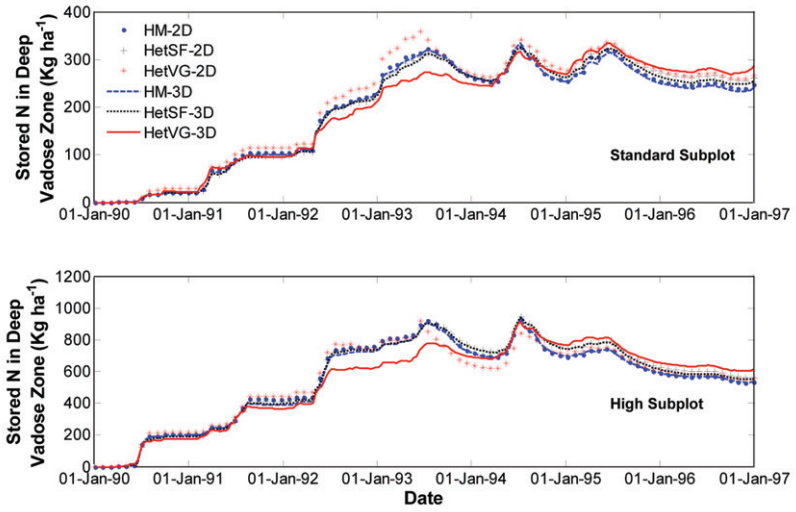

Fig. 14. Total nitrate N mass simulated in the deep vadose zone of the standard and high subplots during the period from 1990 to 1996 in the homogeneous and heterogeneous lithofacies models.

that include lithofacies and local heterogeneity. The root zone mass balance approach yields a total N mass in the deep vadose of 261 kg N ha^{-1} for the standard subplot and 478 kg N ha^{-1} for the high subplot. This is also largely consistent with the numerical modeling results.

The geologically and texturally highly variable vadose zone, when represented in numerical models, induces strongly heterogeneous flow patterns within the vadose zone (Fig. 11, 13) as shown previously in many theoretical studies (e.g., Hopmans et al., 1988; Ünlü et al., 1990; Kung, 1993; Russo, 1991; Harter and Yeh, 1996; Harter et al., 1996; Roth and Hammel, 1996). When comparing simulated concentration profiles from single solute injection events (e.g., Russo, 1991, Harter and Yeh, 1996; Roth and Hammel, 1996) to those in our simulations with repeated solute applications (Fig. 13), the variability in solute flux and concentration is in qualitative agreement across various conceptual and numerical simulation methods that include representation of local-scale sediment heterogeneity.

The simulated patterns of the nitrate distribution for the HetSF and HetVG models of the deep vadose zone are qualitatively in striking similarity to those inferred from field site data (compare Fig. 13 with Fig. 9 in Onsoy et al., 2005). The relative concentration distribution produced by these four models (but not by the HM model) is also consistent with the measured field nitrate correlation lengths of less than 1 m horizontally and several meters vertically (see Fig. 8 in Onsoy et al., 2005).

Despite these similarities in concentration patterns between HetSF, HetVG, and the field site, the variability in downward velocity across the heterogeneous soil profile (Fig. 11) is not sufficient to significantly alter the strong control that large, transient but cyclical root zone water losses (net recharge rate) and nitrate leaching have on water table nitrate flux below this thick unsaturated zone. For non-reactive solute transport under near-cyclical steady state loading, the field scale, long-term average water table flux of nitrate appears, in fact, to be well approximated by simple mass balance and plug flow, which gives similar travel times and mass flux to the more complex, heterogeneous numerically-based models, even if it is a conceptually radical oversimplification of the type of nitrate distribution found in the deep vadose zone at our field site.

Two-dimensional vs. Three-Dimensional Simulation Domains

In the numerical simulations, the extension of the model dimensionality into the third dimension did not prove to have much effect on model predictions of long-term nitrate losses to groundwater and their timing, except for the HetVG-3D simulation which has noticeable higher N uptake (Fig. 6) and lower N

flux to the water table (Fig. 8) than corresponding two-dimensional simulations. These differences are thought to stem from the higher complexity of three-dimensional porous media, which moves more nitrate into lower permeable zones in the root zone than would be the case in two-dimensional porous media. This increases the incidence of N uptake and decreases cumulative N mass reaching the water table over time.

Measured vs. Simulated Deep Vadose Zone Nitrogen Mass

Both, the plug flow approach (coupled with the root zone mass balance) and the heterogeneous numerical models fail to characterize field observations in two important aspects. First, all estimates severely overestimate the measured N mass in the deep vadose zone. For the highly heterogeneous geology of the alluvial sediments observed at the orchard site (Onsoy et al., 2005), neither uniform plug flow in the deep vadose zone, nor the heterogeneous models provide an adequate conceptual framework for explaining the observed fate of nitrate in the nearly 16-m deep vadose zone.

Second, not even the most heterogeneous (HetVG-3D) of the six models provide an adequate prediction of the total nitrate variance observed at the field site (Onsoy et al., 2005), despite the fact that the large degree of physical hydraulic heterogeneity measured in the field was directly incorporated into these numerical models.

The low N mass encountered at the field site could be due to significant denitrification. However, field data indicate that nitrate and nitrate-^{15}N isotope concentration profiles, while variable, show no measurable trend along the vertical profile (Onsoy et al., 2005; Harter et al., 2005). Denitrification losses in the root zone may reduce total annual nitrate loading to below the root zone by 5 to 15%, given field studies under similar climate, soil, and moisture conditions (Onsoy et al., 2005). The low N mass encountered in the deep vadose zone at the site (~13– 17% of simulated) is therefore largely attributed to rapid or preferential flow conditions. Accordingly, these are thought to transport nitrate ~6–8 times faster, with a corresponding decrease in travel time and mass stored in the vadose zone, at any given time.

Close examination of the site's subsurface texture strongly suggested that wetting front instability (de Rooij, 2000) was present at the site, at least in some lithofacies. Wetting front instability creates unstable, preferential flows in a variety of settings in both uniform (Glass et al., 1991; Wang et al., 1998, Wang et al., 2003a) and layered soil systems (Flury et al., 1994; Steenhuis et al., 1998; Wang et al., 2003b). Furthermore, extrinsic factors such as irrigation management and fertilizer applications were found to contribute much to variability in water fluxes and nitrate concentrations (Böhlke, 2002). Near the surface, water repellency of the sandy loam is conducive to preferential flow into the subsoil as demonstrated by Wang et al. (2003b). Ritsema et al. (1998) estimated that more than 80% of infiltrating water during a rain storm event was transported in preferential flow paths through a water repellent soil to the deep subsoil. Furthermore, most of non-detect nitrate samples occurred in a thick sand facies at 7- to 10-m depth, at locations with high saturated hydraulic conductivity and small air-entry pressure, and therefore conducive to preferential flow (Wang et al., 2004).

Of particular concern is the fact, that the models, despite strongly varying velocity fields, were unable to reproduce actual field nitrate variability in the range of 0.02 mg L^{-1} (field detection limit) to 3.9 mg L^{-1} (lowest simulated concentration in 1997, corresponding to the time of the field sampling campaign). However, low concentrations contrasts in the simulations are to be expected physically:

First and most importantly, simulated velocity contrasts are not sufficiently high to shield significant portions of the deep vadose zone from significant downward flow during the summer irrigation season. Relatively large sections of the flow domain experience downward velocities of at least 2 cm d^{-1} for some portion of the season (Fig. 11); thus, allowing for widespread penetration of frequent nitrate pulses. The fastest simulated flow paths appear to be spaced from one to a few meters apart, with a typical width corresponding to the finite difference cell width (20–30 cm) or slightly larger. The resulting patches of high nitrate concentration at depth are spaced apart similarly. This is consistent with field observations yielding nitrate semi-variograms with horizontal correlation lengths of 1 m or less (Onsoy et al., 2005).

Second, over a period of five to 10 yr (the orchard was 22-yr-old at the time of sampling), diffusion of nitrate ($D = 1.7\ 10^{-9}$ m^2 s^{-1}, Picioreanu et al., 1997) within a continuous water phase increases the concentration at 1 m distance from a constant concentration boundary, to 17–34% of the boundary concentration. Here, the boundary could be a high flow path with frequently high nitrate concentrations. Physically, we would therefore expect the long-term cyclical boundary conditions of this experiment to work against large nitrate contrasts to persist in time, even in the deep vadose zone (under the site-specific high recharge conditions). In the simulations, numerical transverse dispersion of the finite difference model is significantly higher than the natural nitrate diffusion rate considered above, thus further dampening simulated concentration contrasts.

Hence, besides the presence of preferential flow paths, partly achieved by the HetSF and HetVG models, comparison of field results with our physical models infers that significant barriers exist to transverse dispersion and diffusion into regions with very low (or no) flow. Rimon et al. (2011) provided significant field evidence supporting the concept of a dual domain flow and transport system in soils, with no significant diffusion between the two domains.

Dividing the pore space of the unsaturated zone conceptually into an isolated immobile domain and mobile domain provides a

parsimonious model representation of preferential or dual domain flow within the context of our observed heterogeneity and conceptual models described above. If we further assume that diffusive solute transfer between the mobile and immobile domain is negligibly small (*ibid.*), we can readily obtain the immobile fraction of the deep vadose zone at the Kearney site by calibrating the simulated deep vadose zone N mass, m_{sim}, against the measured deep vadose zone N mass, m_{meas}. The calibrated fraction of the immobile domain (as a fraction of average moisture content) is $100(1-m_{meas}/\mu_{sim})\%$, where μ_{sim} is the simulated mass of the single flow domain simulations given above. The calibrated fraction of the immobile domain (effectively void of nitrate or with very low nitrate concentrations) ranges from 83 to 87% for the six different simulation approaches (13 to 17% mobile domain). The effective nitrate travel time through the entire deep vadose zone within the remaining mobile domain is about 6 mo. This is consistent with qualitative observations of rapid rewetting to about 10-m depth within 14 d of an irrigation that occurred during the core drilling process. The significant size of the effectively immobile domain would explain the significant proportion of measured low concentrations. The much higher concentration variability observed in the field, when compared to the simulated concentrations, suggests that the effectively immobile space is distributed non-uniformly throughout the vadose zone at length-scales as large as the field sample spacing (decimeters to meters, see Fig. 9 in Onsoy et al., 2005) rather than only at length scales comparable to pore size (e.g., Rimon et al., 2011). However, further field research is needed to directly measure and characterize such immobile regions or regions of inactive nitrate transport.

Conclusions

This study provides multiple detailed, multi-year transient simulation results of nitrate transport in a deep vadose zone using and comparing several complex vadose zone models that represent variability using key conceptual approaches for flow and transport in the unsaturated zone that have been developed over the past three decades. The work is based on the Kearney field site, which offers a rich database for detailed geologic, hydraulic, and chemical characterization of the deep vadose zone stratigraphy that is typical for alluvial sediments in the eastern San Joaquin Valley, California. The site database provides a foundation for the development and validation of alternative modeling tools to assess the potential for nitrate leaching to groundwater in the presence of a deep, heterogeneous vadose zone at the site.

The set of modeling tools conceptually represents recent advances in stochastic modeling approaches. Both, the simple root zone mass balance model and the two-dimensional and three-dimensional numerical models used in this study are found limited in their ability to predict the low total nitrate mass measured in the deep vadose zone or the large variability of nitrate observed in the deep vadose zone at the field site. One possible explanation for the discrepancy is that highly non-uniform conditions control flow and nitrate transport at the Kearney site. Yet, within the framework of Richards flow equation and the advection-dispersion equation, and despite applying highly heterogeneous parameters, we find that diffusive water flow and solute dispersion, and the strong mass flux control at the upper boundary counterbalance the high heterogeneity of the soil and the resulting highly variable flux field in the simulated advective transport of nitrate. Our hypothesis that a full accounting of small scale heterogeneity in the simulation of flow based on the Richards equation would explain the low nitrogen mass stored in the vadose zone has been disproven. This is consistent with de Rooij (2000), Simunek et al. (2003), and Gärdenäs et al. (2006) who showed that Richards equation may be an inadequate model as it generally leads to relatively uniform flow and transport behavior, especially at field sites with repeated solute applications.

Incorporating other conceptual models such as dual porosity or mobile-immobile flow domains may be necessary to account for strong non-equilibrium non-uniform flow and transport not properly captured by the constitutive equations used here. Our field measurements provide sufficient evidence to support use of these types of models. However, additional field work will be needed to confirm the appropriateness of such modeling approaches.

Other conceptual elements that require more field data before further model development include spatially variable denitrification, e.g., high denitrification rates in stagnant zones of water flow but not in preferential flow paths (similar to, for example, the concepts proposed by Tartakovsky et al., 2008). Sampled data show no significant increase of nitrate-^{15}N isotope concentration with depth, which would be indicative of deep vadose zone denitrification. However, this does not rule out the existence of high denitrification rates in stagnant zones that do not contribute to increased nitrate-^{15}N isotope concentrations in the mobile flow zone with increasing depth due to complete denitrification.

Regardless of shortcomings in explaining the low nitrogen mass in deep vadose zone, this study further confirms and illustrates some important findings:

- The transient behavior of precipitation, irrigation, and evapotranspiration at the land surface affects not only the root zone, but rapidly affects moisture and water flux throughout a 16-m thick unsaturated zone. All of these are shown to be highly transient, even at the water table, under the irrigated, semiarid conditions investigated here and typical for agricultural regions in semiarid climates.
- Low irrigation efficiencies (on the order of 45–65%) contribute not only to significant leaching of fertilizer, but also to rapid transport of nitrate to groundwater. At the field site, irrigated at relatively low irrigation efficiencies, the travel time to groundwater through the 16-m thick vadose zone is predicted (based on the three models) to be as short as 2.5–3.5 yr and, after taking into account potential preferential flow, may be as short

as a few months. By the same token, higher irrigation efficiencies would result in significantly longer travel times.

- In situations where the Richards equation is to be used under strong infiltration conditions using relatively large numerical grid blocks, results show relatively uniform flow and transport behavior at the field scale, regardless of the level of heterogeneity incorporated.
- Under irrigated conditions with low irrigation efficiency (or under conditions of frequent rainfall) and repeated solute applications, the field scale simulation of solute mass transfer through deep, heterogeneous unsaturated zones with complex stochastic methods representing high local scale heterogeneity will yield results that are, practically speaking, not unlike those from simple mass balance and a plug flow conceptualization.

Future work needs to further explore mechanisms responsible for generating the highly heterogeneous, yet relatively low mass nitrate concentration profile found at the investigated field site; and similar detailed characterization work of deep vadose zones at other field sites is needed to further confirm or reject the hypothesis that these conditions are potentially wide-spread in unconsolidated sedimentary, deep vadose zones.

Acknowledgments

This work was performed with funding support from the University of California Kearney Foundation of Soil Sciences.

References

Allaire-Leung, S.E., L. Wu, J.P. Mitchell, and B.L. Sanden. 2001. Nitrate leaching and soil nitrate content as affected by irrigation nonuniformity in a carrot field. Agric. Water Manage. 48:37–50. doi:10.1016/S0378-3774(00)00112-8

Allen, R.G., L.S. Pereira, D. Raes, and M. Smith. 1998. FAO Irrigation and Drainage Paper. No. 56. Crop evapotranspiration. FAO of the United Nations, Rome, Italy, p. 300

Baran, N., J. Richert, and C. Mouvet, 2007. Field data and modeling of water and nitrate movement through deep unsaturated loess. J. Hydrol. 345: 27–37. doi:10.1016/j.jhydrol.2007.07.006

Biggar, J.W., and D.R. Nielsen. 1978. Field monitoring of soil water constituents in the unsaturated zone. In L.G. Everett and K.D. Schmidt, editors, Establishment of Water Quality and Monitoring Programs. Proc. Am. Water Resources Assoc., San Francisco, Ca. 12–14 June 1978. Tech. Publ. Ser. No.TPS79–1. Am. Water Resour. Assoc., Minneapolis, MN, p. 106–121.

Böhlke, J.-K. 2002. Groundwater recharge and agricultural contamination. Hydrogeol. J. 10:153–179. doi:10.1007/s10040-001-0183-3

Botros, F. E., T. Harter, Y. S. Onsoy, M. Denton, A. Tuli, and J.W. Hopmans, 2009. Spatial variability of hydraulic propertiesand sediment characteristics in a deep alluvial unsaturated zone. Vadose Zone J. 8:276–289.doi: 10.2136/vzj2008.0087

Braud, I., A.C. Dantas-Antonio, and M. Vauclin. 1995. A stochastic approach to studying the influence of the spatial variability of soil hydraulic properties on surface fluxes, temperature, and humidity. J. Hydrol. 165(1–4):283–310. doi:10.1016/0022-1694(94)02548-P

Brooks, R.H., and A.T. Corey. 1964. Hydraulic properties of porous media. Hydrol. Papers 3. Colo. State Univ., Fort Collins, CO. p. 27.

Celia, M.A., E.T. Bouloutas, and R.L. Zarba. 1990. A general mass-conservative numerical solution for the unsaturated flow equation. Water Resour. Res. 26(7):1483–1496. doi:10.1029/WR026i007p01483

deRooij, G.H. 2000. Modeling fingered flow of water in soils owing to wetting front instability: A review. J. Hydrol. 231–232:277–294. doi:10.1016/S0022-1694(00)00201-8

deVos, J.A., D. Hesterberg, and P.A.C. Raats. 2000. Nitrate leaching in a tiled-drained silt loam soil. Soil Sci. Soc. Am. J. 64:517–527. doi:10.2136/sssaj2000.642517x

Doorenbos, J., and W.O. Pruitt. 1977. Crop water requirements. Rev. 1977. FAO Irrig. And Drain. Paper 24, FAO of the United Nations, Rome, p. 144.

Dubrovsky, N.M., K.R. Burow, G.M. Clark, J.M. Gronberg, P.A. Hamilton, K.J. Hitt, D.K. Mueller, M.D. Munn, B.T. Nolan, L.J. Puckett, M.G. Rupert, T.N. Short, N.E. Spahr, L.A. Sprague, and W.G. Wilber. 2010. Nutrients in the Nation's Streams and Groundwater, 1992–2004. Geol. Surv. Circ. No.1350, USGS, Reston, VA.

DWR. 2001. Crop water use. San Joaquin District Report. Department of Water Resources, Sacramento, CA.

Eching, S.O., and J.W. Hopmans. 1993. Optimization of hydraulic functions from transient outflow and soil water pressure head data. Soil Sci. Soc. Am. J. 57:1167–1175. doi:10.2136/sssaj1993.03615995005700050001x

Feddes, R.A., P.J. Kowalik, and H. Zaradny. 1978. Simulation of field water use and crop yield. Simulation Monographs, Pudoc, Wageningen, The Netherlands. p. 188.

Flury, M., H. Flühler, W.A. Jury, and J. Leuenberger. 1994. Susceptibility of soils to preferential flow of water: A field study. Water Resour. Res. 30(7):1945–1954. doi:10.1029/94WR00871

Gärdenäs, A., J. Šimunek, N. Jarvis, and M.Th. van Genuchten. 2006. Two-dimensional modeling of preferential water flow and pesticide transport from a tile-drained field. J. Hydrol. 329:647–660. doi:10.1016/j.jhydrol.2006.03.021

Gardner, W.R. 1958. Some steady state solutions of unsaturated moisture flow equations with application to evaporation from a water table. Soil Sci. 85(4):228–232. doi:10.1097/00010694-195804000-00006

Glass, R.J., J.-Y. Parlange, and T.S. Steenhuis. 1991. Immesible displacement in pororus media: Stability analysis of three-dimensional, axisymmetric disturbances with application to gravity-driven wetting front instability. Water Resour. Res. 27(8):1947–1956. doi:10.1029/91WR00836

Harter, T., and T.-C.J. Yeh. 1996. Stochastic analysis of solute transport in heterogeneous, variably saturated soils. Water Resour. Res. 32(6):1585–1595. doi:10.1029/96WR00502

Harter, T., A.L. Gutjahr, and T.-C.J. Yeh. 1996. Linearized cosimulation of hydraulic conductivity, pressure head, and flux in saturated and unsaturated, heterogeneous porous media. J. Hydrol. 183:169–190. doi:10.1016/S0022-1694(96)80040-0

Harter, T., and T.C.J. Yeh. 1998. Flow in unsaturated random porous media, nonlinear numerical analysis, and comparison to analytic stochastic models. Adv. Water Resour. 22(3):257–272. doi:10.1016/S0309-1708(98)00010-4

Harter, T., K. Heeren, G. Weissmann, W.R. Horwath, and J.W. Hopmans. 1999. Field scale characterization of a heterogeneous, moderately deep vadose zone: The Kearney Research Site, Proceedings, Characterization and Measurement of the Hydraulic Properties of Unsaturated Porous Media, United States Salinity Laboratory, Riverside, CA, p. 621–630.

Harter, T., Y.S. Onsoy, K. Heeren, M. Denton, G. Weissmann, J.W. Hopmans, and W.R. Horwath. 2005. Deep vadose zone hydrology demonstrates fate of nitrate in eastern San Joaquin Valley. Calif. Agric. 59(2):124–132. doi:10.3733/ca.v059n02p124

Harter, T., J.R. Lund, J. Darby, G.E. Fogg, R. Howitt, K.K. Jessoe, G.S. Pettygrove, J.F. Quinn, J.H. Viers, D.B. Boyle, H.E. Canada, N. DeLaMora, K.N. Dzurella, A. Fryjoff-Hung, A.D. Hollander, K.L. Honeycutt, M.W. Jenkins, V.B. Jensen, A.M. King, G. Kourakos, D. Liptzin, E.M. Lopez, M.M. Mayzelle, A. McNally, J. Medellin-Azuara, and T.S. Rosenstock. 2012. Addressing nitrate in California's drinking water with a focus on Tulare Lake basin and Salinas Valley groundwater. Report for the State Water Resources Control Board Report to the Legislature. Center for Watershed Sciences, University of California, Davis.http://groundwaternitrate.ucdavis.edu.

Haverkamp, R., M. Vaclin, J. Touma, P.J. Wierenga, and G. Vachaud. 1977. A comparison of numerical simulation models for one-dimensional infiltration. Soil Sci. Soc. Am. J. 41:285–294. doi:10.2136/sssaj1977.03615995004100020024x

Hills, R.G., P.J. Wierenga, D.B. Hudson, and M.R. Kirkland. 1991. The second Las Cruces trench experiment: Experimental results and two-dimensional flow predictions. Water Resour. Res. 27(10):2707–2718. doi:10.1029/91WR01538

Hopmans, J.W., and K.L. Bristow. 2002. Current capabilities and future needs of root water and nutrient uptake modeling. Adv. Agron. 77:103–183. doi:10.1016/S0065-2113(02)77014-4

Hopmans, J.W., H. Schukking, and P.J.J.F. Torfs. 1988. Two-dimensional steady state unsaturated water flow in heterogeneous soils with autocorrelated soil hydraulic properties. Water Resour. Res. 24(12):2005–2017. doi:10.1029/WR024i012p02005

Johnson, R.S., F.G. Mitchell, and C.H. Crisosto. 1995. Nitrogen fertilization of Fantasia nectarine–A 12-year study. UC Kearney Tree Fruit Rev. 1:14–19.

Jury, W.A., D. Russo, G. Sposito, and H. Elabd. 1987. The spatial variability of water and solute transport properties in unsaturated soil: II. Scaling models of water transport. Hilgardia 55:33–56.

Klute, A. (ed.). 1986. Methods of soil analysis. Part 1: Physical and mineralogical methods. 2nd ed. American Society of Agronomy, Soil Science Society of America, Madison, WI, p. 1188.

Kung, K.-J.S. 1993. Laboratory observation of the funnel flow mechanism and its influence on solute transport. J. Environ. Qual. 22:91–102. doi:10.2134/jeq1993.00472425002200010012x

Lafolie, F., L. Bruckler, and A.M. de Corkborne. 1997. Modeling the water transport and nitrogen dynamics in irrigated salad crops. Irrig. Sci. 17:95–104. doi:10.1007/s002710050027

Ling, G., and A.I. El-Kadi. 1998. A lumped parameter model for nitrogen transformation in the unsaturated zone. Water Resour. Res. 34(2):203–212. doi:10.1029/97WR02683

Martin, D.L., J.R. Gilley, and R.W. Skaggs. 1991. Soil water balance and management. In R.F. Follett et al., editors, Managing Nitrogen for Groundwater Quality and Farm Profitability. Soil Science Society of America, , Madison, WI, p. 199–235.

Miller, E.E., and R.D. Miller. 1956. Physical theory for capillary flow phenomena. J. Appl. Phys. 27(4):324–332. doi:10.1063/1.1722370

Mualem, Y. 1976. A new model for predicting the hydraulic conductivity of unsaturated porous media. Water Resour. Res. 12:513–522. doi:10.1029/WR012i003p00513

Nimmo, J.R., J.A. Deason, J.A. Izbicki, and P. Martin. 2002. Evaluation of unsaturated zone water fluxes in heterogeneous alluvium at a Mojave Basin Site. Water Resour. Res. 38(10):1215–1228. doi:10.1029/2001WR000735

Oliveira, L.I., A.H. Demond, L.M. Abriola, and P. Goovaerts. 2006. Simulation of solute transport in a heterogeneous vadose zone describing the hydraulic properties using a multistep stochastic approach. Water Resour. Res. 42(5):W05420.doi:10.1029/2005WR004580

Onsoy, Y.S. 2005. Modeling nitrate transport in deep unsaturated alluvial sediments and assessing impact of agricultural management practices on groundwater quality. Ph.D. diss. Univ. California, Davis, Davis, CA.

Onsoy, Y.S., T. Harter, T. Ginn, and W. Horwath. 2005. Spatial variability and transport of nitrate in a deep alluvial vadose zone. Vadose Zone J. 4:41–51. doi:10.2113/4.1.41

Pan, F., M. Ye, J. Zhu, Y.S. Wu, B. Hu, and Z. Yu. 2009. Incorporating layer- and local-scale heterogeneities in numerical simulation of unsaturated flow and tracer transport. J. Contam. Hydrol. 103(3–4):194–205.doi:10.1016/j.jconhyd.2008.10.012

Picioreanu, C., M.C.M. Van Loosdrecht, and J.J. Heijnen. 1997. Modeling the effect of oxygen concentration on nitrite accumulation in a biofilm airlift suspension reactor. Water Sci. Technol. 36(1):147–156. doi:10.1016/S0273-1223(97)00347-8

Rao, P.S.C., and R.J. Wagenet. 1985. Spatial variability of pesticides in field soils: Methods for data analysis and consequences. Weed Sci. 33(2):18–24.

Rassam, D., J. Simunek, and M.Th. van Genuchten. 2003. Modeling variably saturated flow with HYDRUS-2D.1st ed. ND Consult, Brisbane, Australia.

Rimon, Y., R. Nativ, and O. Dahan. 2011. Physical and chemical evidence for pore-scale dual-domain flow in the vadose zone. Vadose Zone J. 10:322–331. doi:10.2136/vzj2009.0113

Ritsema, C.J., L.W. Dekker, J.L. Nieber, and T.S. Steenhuis. 1998. Modeling and field evidence of finger formation and finger recurrence in a water repellent sandy soil. Water Resour. Res. 34(4):555–567. doi:10.1029/97WR02407

Rockhold, M., R. Rossi, and R. Hills. 1996. Application of similar media scaling and conditional simulation for modeling water flow and Tritium transport at the Las Cruces Trench Site. Water Resour. Res. 32(3):595–609. doi:10.1029/95WR03398

Rockhold, M.L., C.S. Simmons, and M.J. Fayer. 1997. An analytical solution technique for one-dimensional, steady vertical water flow in layered soils. Water Resour. Res. 33(4):897–902. doi:10.1029/96WR03746

Roth, K. 1995. Steady state flow in an unsaturated, two-dimensional, macroscopically homogeneous, Miller-similar medium. Water Resour. Res. 31(9):2127–2140. doi:10.1029/95WR00946

Roth, K., and K. Hammel. 1996. Transport of conservative chemical through and unsaturated two-dimesnional Miller-similar medium with steady state flow. Water Resour. Res. 32(6):1653–1663. doi:10.1029/96WR00756

Roth, K., W.A. Jury, H. Fluhler, and W. Attinger. 1991. Transport of chloride through a vadose field soil. Water Resour. Res. 27(10):2533–2541. doi:10.1029/91WR01771

Russo, D. 1988. Determining soil hydraulic properties by parameter estimation: On the selection of a model for the hydraulic properties. Water Resour. Res. 24:453–459. doi:10.1029/WR024i003p00453

Russo, D. 1991. Stochastic analysis of simulated vadose zone solute transport in a vertical cross section of heterogeneous soil during nonsteady water flow. Water Resour. Res. 27(3):267–283. doi:10.1029/90WR02105

Scheidegger, A.L. 1960. The physics of flow through porous media. University of Toronto Press, Toronto.

Seong, K., and Y. Rubin. 1999. Field investigation of the waste isolation pilot plant (WIPP) site (New Mexico) using a nonstationary stochastic model with a trending hydraulic conductivity field. Water Resour. Res. 35(4):1011–1018. doi:10.1029/1998WR900107

Sheldrick, B.H., and C. Wang. 1993. Particle size distribution. In M.R. Carter, editor, Soil sampling and methods of soil analysis. Lewis Publishers, Boca Raton, FL, p. 499–512.

Simunek, J., and J.W. Hopmans. 2009. Modeling compensated root water and nutrient uptake. Ecol. Modell. 220(4):505–521. doi:10.1016/j.ecolmodel.2008.11.004

Simunek, J., T. Vogel, and M.Th. van Genuchten. 1996. HYDRUS-2D code for simulating water flow and solute transport in two-dimensional variably saturated media. Version 1.0. USDA/ARS, U.S. Salinity Lab., Riverside, CA.

Simunek, J., N.J. Jarvis, M.Th. van Genuchten, and A. Gardenas. 2003. Review and comparison of models for describing non-equilibrium and preferential flow and transport in the vadose zone. J. Hydrol. 272:14–35. doi:10.1016/S0022-1694(02)00252-4

Steenhuis, T., K. Vandelheuvel, K.W. Weiler, J. Boll, J. Daliparthy, S. Herbert, and K.-J.S. Kung. 1998. Mapping and interpreting soil textural layers to assess agri-chemical movement at several scales along the eastern seaboard (USA). Nutr. Cycl. Agroecosyst. 50:91–97. doi:10.1023/A:1009711521793

Stenger, R., E. Priesack, and F. Beese. 2002. Spatial variation of nitrate-N and related soil properties at the plot scale. Geoderma 105:259–275. doi:10.1016/S0016-7061(01)00107-0

Tartakovsky, A.M., G. Redden, P.C. Lichtner, T.D. Scheibe, and P. Meakin. 2008. Mixing-induced precipitation: Experimental study and multiscale numerical analysis. Water Resour. Res. 44:W06S04. doi:10.1029/2006WR005725

Troiano, J., C. Garretson, C. Krauter, J. Brownell, and J. Huston. 1993. Influence of amount and method of irrigation water application on leaching of atrazine. J. Environ. Qual. 22(2):290–298. doi:10.2134/jeq1993.00472425002200020009x

Tseng, P.-H., and W.A. Jury. 1994. Comparison of transfer function and deterministic modeling of area-averaged solute transport in a heterogeneous field. Water Resour. Res. 30(7):2051–2064. doi:10.1029/94WR00752

United Nations. 2011. "Report of the Special Rapporteur on the human right to safe drinking water and sanitation, Catarina de Albuquerque," UN General Assembly Report A/HRC/18/33/Add.4. http://www2.ohchr.org/english/bodies/hrcouncil/docs/18session/A-HRC-18-33-Add4_en.pdf. (accessed 30 Oct. 2011).

Ünlü, K., D.R. Nielsen, and J.W. Biggar. 1990. Stochastic analysis of vadose flow: One-dimensional Monte Carlo simulations and comparisons with spectral perturbation analysis and field observations. Water Resour. Res. 26(9):2207–2218.

Ünlü, K., G. Ozenirler, and C. Yurteri. 1999. Nitrogen fertilizer leaching from cropped and irrigated sandy soil in Central Turkey. Eur. J. Soil Sci. 50:609–620. doi:10.1046/j.1365-2389.1999.00260.x

Vachaud, G., M. Vauclin, and P. Balabanis. 1988. Stochastic approach of soil water flow through the use of scaling factors: Measurement and simulation. Agric. Water Manage. 13:249–261. doi:10.1016/0378-3774(88)90158-8

van Genuchten, M.Th. 1980. A closed form equation for predicting the hydraulic conductivity of unsaturated soils. Soil Sci. Soc. Am. J. 44:892–898. doi:10.2136/sssaj1980.03615995004400050002x

Vogeler, I., S.R. Green, D.R. Scotter, and B.E. Clothier. 2001. Measuring and modeling the transport and root uptake of chemicals in the unsaturated zone. Plant Soil 231:161–174. doi:10.1023/A:1010337132309

Wagenet, R.J., and J.L. Hutson. 1989. LEACHM: A process-based model for water and solute movements, transformations, plant uptake and chemical reactions in the unsaturated zone, version 2.0., Vol. 2, New York State Water Resources Institute, Cornell University, Ithaca, NY.

Wang, Z., J. Feyen, and C.J. Ritsema. 1998. Susceptibility and predictability of conditions for preferential flow. Water Resour. Res. 34(9):2169–2182. doi:10.1029/98WR01761

Wang, Z., A. Tuli, and W.A. Jury. 2003a. Unstable flow during distribution in homogeneous soil. Vadose Zone J. 2:52–60.doi: 10.2113/2.1.52

Wang, Z., L. Wu, T. Harter, J. Lu, and W. A. Jury, 2003b. A field study of unstable preferential flow during soil water redistribution. Water Resour. Res., 39(4):1075–1089. doi:10.1029/2001WR000903

Wang, Z., W.A. Jury, A. Tuli, and D. Kim. 2004. Unstable flow during redistribution: Controlling factors and practical implications. Soil Sci. Soc. Am. J. 3:549–559.doi: 10.2113/3.2.549

Warrick, A.W., G.J. Mullen, and D.R. Nielsen. 1977. Scaling field measured soil hydraulic properties using a similar media concept. Water Resour. Res. 13(2):355–362. doi:10.1029/WR013i002p00355

Weinbaum, S.A., R.S. Johnson, and T.M. DeJong. 1992. Causes and consequences of overfertilization in orchards. Hort Technol. 2(1):112–119.

Zavattaro, L., N. Jarvis, and L. Persson. 1999. Use of similar media scaling to characterize spatial dependence of near-saturated hydraulic conductivity. Soil Sci. Soc. Am. J. 63:486–492. doi:10.2136/sssaj1999.03615995006300030010x

Zhu, J., and B.P. Mohanty. 2002. Upscaling of soil hydraulic properties for steady state evaporation and infiltration. Water Resour. Res. 38(9):1178–1191. doi:10.1029/2001WR000704